WEDNESDAY SLIDE CONFERENCE 2021-2022

Conference 10

1 December 2021

<u>**CASE I:**</u> N2018-0119 (JPC 4153147)

Signalment:
Adult, female, Sambava tomato frog (*Dyscophus guineti)*

History:
This Sambava tomato frog was found dead during routine morning rounds with no adverse clinical history.

Gross Pathology:
Extending from the rostral maxillary mucosa of the left internal naris is an approximately 3 mm thick x 2 mm diameter, pink and smooth mass.

Laboratory results:
No laboratory findings reported.

Microscopic Description:
Extending from two representative sections of the left maxillary oral mucosa is an unencapsulated, variably well-demarcated, exophytic, and moderately cellular mass composed of two distinct populations of epithelial and mesenchymal cells forming multiple tooth-like structures (denticles) embedded within a pre-existing stroma. Denticles range from 50 to 250 microns in diameter and are composed of a combination of eosinophilic, homogenous to fibrillar material (dentin), palisading epithelium with apical nuclei and basilar cytoplasmic clearing (odontogenic epithelium; ameloblasts), and proliferating mesenchymal cells with small and hyperchromatic nuclei (odontoblasts). Central arcs of dentin are frequently lined by ameloblasts along their convex surface and odontoblasts along their concave surface. No mitoses are identified, and anisocytosis and anisokaryosis are minimal. Rare individual lymphocytes and plasma cells multifocally infiltrate the mass.

Contributor's Morphologic Diagnoses:
Gingival mass: Odontoma, compound type

Contributor's Comment:
Odontomas are odontogenic tumors with variably organized dental elements; they are designated as complex or compound based on how closely they parallel tooth


Figure 1-1. Cross section through head, tomato frog. Hemisections of mandible (top) and a cross section of the head (bottom) are submitted for examination. (HE, 5X)

embryogenesis. Familiarity with normal early tooth development is thus essential in accurate classification of odontomas, in addition to odontogenic lesions in general.

Two tissue types are involved in mammalian odontogenesis: odontogenic epithelium and ectomesenchyme. The process initiates as ectoderm-derived oral epithelium extends into underlying connective tissue, forming a bud of epithelium referred to as the dental lamina (bud stage).[8] As the dental lamina expands, it induces adjacent neural crest-derived ectomesenchyme to proliferate and differentiate into the dental papilla, which organizes along a concavity of the dental lamina and is the future source of dental pulp and odontoblasts (cap stage). Next, a bell-like structure forms from continued proliferation of oral epithelium, which differentiates into the enamel organ, composed of central stellate reticulum, inner ameloblasts and stratum intermedium, and outer ameloblasts (bell stage). The underlying ectomesenchyme condenses and forms a dental follicle; the precursor to the periodontal ligament. As time progresses, production of dental matrix begins by differentiated odontoblasts of the dental papilla, which produce predentin that calcifies to dentin. This then leads to the crown stage, where ameloblasts produce overlying enamel.
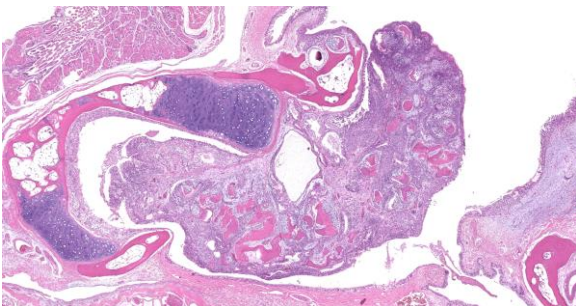
Figure 1-2. Maxilla, tomato frog. An exophytic mass from the oral submucosa projects into the oral cavity. At this magnification, the mass is composed of disorganized trabeculae of columnar epithelium abutting eosinophilic arcs or islands of dentin. (HE, 30X)
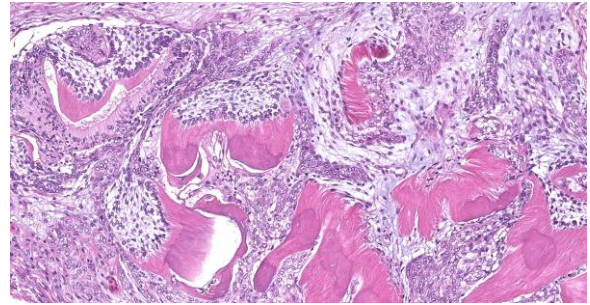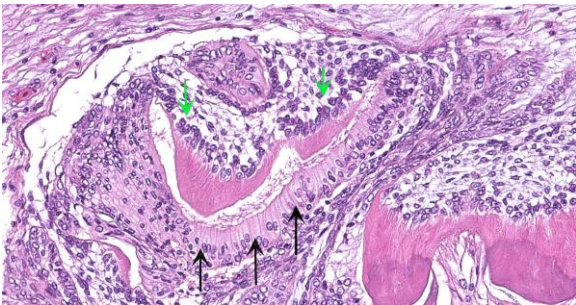

Figure 1-3. Maxilla tomato frog. Higher magnification of the neoplasm demonstrates nests of odontogenic epithelium surrounding crescents of tubular dentin. (HE, 188X)

Complex odontomas are characterized by disorganized conglomerates of odontogenic epithelium, ectomesenchyme of the dental papilla, and dental hard substances (dentin and enamel). Compound odontomas form distinct, tooth-like structures called denticles, where the order of tissues in tooth embryogenesis is generally maintained.[6] A combination of compound and complex structures often exists within a single tumor.[7] Odontomas are uncommon in veterinary species, despite being the most common odontogenic tumor reported in humans, especially children and young adults.[11] They occur most frequently in young dogs and horses, with fewer case reports in other species.[2,4,7] Associated clinical signs generally include unilateral swelling of the face or mandible and displacement of teeth. Although generally benign, they can be locally destructive. Complete surgical excision is typically curative.[9]

Recently, odontomas were reported in three frogs: a Sambava tomato frog (also known as a false tomato frog [*Dyscophus guineti*]), an African clawed frog (*Xenopus laevis*), and a tomato frog of undetermined species.[5] The tumor extended from the maxillary gingiva in all three cases, as occurred in this case. Histologically all tumors formed orderly denticles with ameloblasts, dentin, and odontoblasts, characterizing them as a compound subtype. In one case, the frog was

euthanized due to the presence of the odontoma and the outcomes of the remaining two were unknown (lost to follow-up).

With the exception of members of the family *Bufonidae* who lack teeth, the teeth of anurans are present only on the maxilla.[10] This may explain the predilection for odontomas arising from exclusively the maxillary mucosa in this group. Anurans have polyphyodont and homodont teeth and lack both cementum and a periodontal ligament.[5] Tooth formation in amphibians is similar to that of mammalians, with a few key differences. The posterior teeth may be derived from foregut endoderm, rather than ectoderm.[1] Additionally, prior to meta-morphosis in some amphibians, odontoblasts produce enamaloid, a dentin-like matrix, that is overlain with enamel by ameloblasts.[3] The dental follicle is not histologically apparent in amphibians, which is thought to be related to tooth attachment occurring at the base, rather than the sides, of the teeth.[1] Additionally, the enamel organ in amphibians is described to be comprised of two cell layers – the inner and outer dental epithelium.[3] Whether or not a stellate reticulum and stratum intermedium are additionally present is unclear; reptiles

appear to develop a stellate reticulum, but the latter is often absent in bony fish.[1]

The pathogenesis of odontomas is unknown. Some consider them a type of hamartoma rather than a neoplastic process, and all odontomas are classified as hamartomas in human medicine as of 2017.[7] In the recent report of frogs with odontomas, trauma to the dental lamina leading to de novo dental element formation was proposed.[5]

In the current case, the presence of an odontoma was not considered likely to have contributed to mortality. The animal was in good body condition and the tumor was small enough to not interfere with eating. Based on the identification of odontoma development in multiple frogs, this neoplasm should be considered as a differential diagnosis in cases of oral tumors in anurans.

Contributing Institution:
Wildlife Conservation Society, Zoological Health Program;
https://oneworldonehealth.wcs.org

JPC Diagnosis:
Gingiva: Compound odontoma

JPC Comment:
This case presents an excellent example of an entity commonly associated with domestic species in an exotic animal. In addition, the contributor provides a thorough review of odontogenesis, odontoma classification, and the unique anatomic and developmental features of anurans likely associated with odontoma formation.

With the exclusion of the family *Bufonidae* (toads), the majority of anurans have teeth restricted to the upper jaw, with exception of some hylids in which teeth are also found on the dentary (anterior bone of the lower jaw). Teeth are arranged in a single row on the

Figure 1-4. Maxilla, tomato frog. Formation of a prototooth within the neoplasm. A line of columnar ameloblasts (black arrows) palisades along the convex surface of an irregular crescent of eosinophilic dentin. A line of odontoblasts (green arrows) palisades along its concave surface. Dorsal to the ameloblasts, there is loosely arranged ectomesencyme recapitulating stellate reticulum. (HE, 30X)

paired premaxillaries, maxillaries, and vomers. These homodont bicuspid teeth are very small, measuring less than 1.0 mm long in the northern leopard frog (*Rana pipiens)* but numerous, with up to 184 functional teeth, which are each associated with a replacement tooth, resulting in an average of 368 teeth in this species.[3]

The aquatic larvae of anurans, tadpoles, do not have truly mineralized teeth, with *Xenopus laevis* (African clawed frog) as an exception. Instead, they have horny labial teeth on the upper and lower beak composed of columns of keratinized epithelial cells. Both the number of teeth and the size of the beak grow throughout larval life. Similar to the tail, the keratinized epithelial cells are destroyed by autolysis during meta-morphosis.[3]

The first tooth germs appear during metamorphosis, near the end of hindlimb organogenesis, and the first true teeth are functional after approximately 25 days. Using *R. pipiens* as a model, six dental laminae correspond to the six dentigerous bones, extending lingual to the dental process of each bone and give rise to enamel organs.[3]

In contrast to other anurans, *X. laevis* differs in that true teeth develop in the upper jaw of tadpoles during the last stages of larval life. However, these teeth do not erupt until the end of metamorphosis. The teeth are morphologically similar between larvae and adults but differ size. *X. laevis* teeth form a single row on the upper jaw and are homodont, conical, monocuspid, and slightly curved at the tip.[3]

As noted by the contributor, the cause of odontoma formation in anurans is unknown,

Tumor	Odontogenic epithelium	Stroma	Mesenchyme	Matrix	Species affected	Misc.
Ameloblastoma	Yes	Not essential for diagnosis	None	None	Dog, cat, horse	Keratinization may occur
Amyloid producing odontogenic ameloblastoma	Yes	Not essential for diagnosis	None	Amyloid	Dog, cat, horse	Matrix composed of enamel proteins which are still Congophilic and exhibit apple-green birefringence; IHC + for laminin
Canine acanthomatous ameloblastoma	Yes	Stellate fibroblasts in dense collagen; regularly spaced dilated, empty blood vessels	Periodontal ligament	None	Dog	Interconnected sheets of odontogenic epithelium
Ameloblastic fibroma	Yes	Loose, collagen poor, resembles pulp ectomesenchyme	Pulp ectomesenchyme	None	Young animals, cattle	Most common oral neoplasm in cattle
Ameloblastic fibro-odontoma	Yes	Loose, collagen poor, resembles pulp ectomesenchyme	Pulp ectomesenchyme	Dentin or enamel	Young animals, cattle	
Complex odontoma	Yes	Well-differentiated dentinal tissue	Pulp ectomesenchyme	Dentin, enamel (may be mineralized)	Dog, rodent, primates, horse	Horse, rodents produce cementum; "balls of disorganized dental hard substance"
Compound odontoma	Yes	Well-differentiated dentinal tissue; dense collagen and vascular connective tissue	Pulp ectomesenchyme	Dentin, mineralized enamel	Young dogs	Multiple tooth-like structures (denticles)

Table 1

although trauma to the dental lamina has been hypothesized.[5] The dental lamina is a specialized segment of the embryologic gingival epithelium that invaginates into the developing jaw and gives rise to the enamel organ, a complex structure of odontogenic epithelium that produces enamel. It includes the outer enamel epithelium, stellate reticulum, and inner enamel epithelium.[7] In anurans, the dental lamina is present throughout the life of the animal due to its polyphyodont dentition (i.e. teeth are replaced multiple times throughout the animal's lifetime). Previous studies have demonstrated transplantation of the dental lamina leads to the formation and replication of tooth buds and/or formed teeth, even when transplanted outside the oral cavity.[5] When transplanted along sections of the jaw, tooth development occurs in an orderly fashion with a regular relationship between the teeth and underlying bone.[5]

References:

1. Berkovitz B, Shellis P. Tooth formation. In: *The teeth of non-mammalian vertebrates*. 1st ed. Academic Press;2017:235-254.
2. Brounts SH, Hawkins JF, Lescun TB, Fessler JF, Stiles P, Blevins WE. Surgical management of compound odontomas in two horses. *J Am Vet Med A*. 2004;225(9):1423-1427.
3. Davit-Béal T, Chisaka H, Delgado S, Sire JY. Amphibian teeth: current knowledge, unanswered questions, and some directions for future research. *Biol Rev*. 2007;82:49-81.
4. Hoyer NK, Bannon KM, Bell CM, Soukup JW. Extensive maxillary odontomas in 2 dogs: diagnosis, pathology, and management. *J Vet Dent*. 2016;33(4):234-242.
5. LaDouceur EE, Hauck AM, Garner MM, Cartoceti AN, Murphy BG. Odontomas in frogs. *Vet Pathol.* 2020;57(1):147-150
6. Munday JS, Lohr CV, Kiupel M. Tumors of the alimentary tract. In: Meuten DJ, ed. *Tumors in domestic animals*. 5th ed. Ames, IA: John Wiley; 2017:530-542.
7. Murphy BG, Bell CM, Soukup JW. Odontogenic tumors. In: *Veterinary oral and maxillofacial pathology*. 1st ed. Hoboken, NJ: Wiley-Blackwell; 2020:91-127.
8. Murphy BG, Bell CM, Soukup JW. Tooth development (odontogenesis). In: *Veterinary oral and maxillofacial pathology*. 1st ed. Hoboken, NJ: Wiley-Blackwell; 2020:13-19.
9. Papadimitriou S, Papazoglou LG, Tontis D, Tziafas D, Papaionnnou N, Patsikas MN. Compound maxillary odontoma in a young German shepherd dog. *J Small Anim Pract*. 2005;46:146-150
10. Pessier AP. Amphibia. In: Terio KA, McAloose D, St. Leger J, eds. *Pathology of wildlife and zoo animals*. 1st ed. London, UK: Elsevier; 2018:915–944.
11. Weidner N, Matthews K, Regezi JA. Oral cavity and jaws. In: *Modern surgical pathology*. 2nd ed. Elsevier; 2009:326-362.

CASE II: 73640 (JPC 4166754)

Signalment:
14-year-old female African Penguin, (*Spheniscus demersus*)

History:
This penguin, which was housed in an indoor-outdoor zoological exhibit, presented to veterinary staff for anorexia of 5-days duration. Initial treatments included gavage feeding with Piscivore liquid nutrition, subcutaneous fluids, metoclopramide, maropitant and itraconazole (for possible aspergillosis). Anorexia persisted over the next four days despite supportive care. Four days after presentation, slightly labored breathing was noted, and terbinafine and
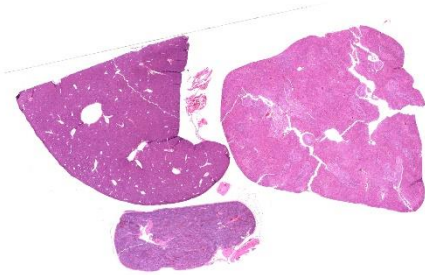
Figure 2-1. Kidney, liver, spleen, penguin. Multiple organs (liver at top left, kidney at top right, and spleen at bottom are submitted for examination; there are no visible lesions at subgross magnification. (HE, 6X)

enrofloxacin were added to the medications. Over the following week, the penguin regurgitated all offered fish, but responded well to gavage feeding and maintained body weight. A radiograph taken on day eight revealed a radiodense foreign body in the caudal ventriculus. Multiple hematology examinations performed during this time showed a decline in hematocrit without overt anemia (PCV remained within reference range) and no signs of infectious or inflammatory disease. While anesthetized for foreign body removal, the bird went into cardiac arrest, and resuscitation efforts were unsuccessful.

Gross Pathology:
At necropsy, the ventriculus contained a bullet measuring 1.5cm in length. The ingesta surrounding the bullet was discolored grey. The mucosal surface appeared intact with no areas of ulceration. The kidneys and other visceral organs appeared grossly un-remarkable.

Laboratory results:
Liver lead level: 48.24 mg/kg
Kidney lead level: 289.5 mg/kg

Microscopic Description:
Kidney – Multifocally, the proximal tubular epithelial cells are mildly swollen with vacuolated cytoplasm and vesicular nuclei (degeneration), or hypereosinophilic and discohesive with pyknotic or lytic nuclei (necrosis). Within the degenerate epithelial cells, nuclei frequently contain multiple, amphophilic, round inclusion bodies measuring approximately 1-3 µm in diameter. Necrotic tubules often contain aggregates of lightly-basophilic, finely gran-ular to radiating, acicular material (consistent with early urate crystal deposition). The intranuclear inclusion bodies are strongly acid-fast positive.
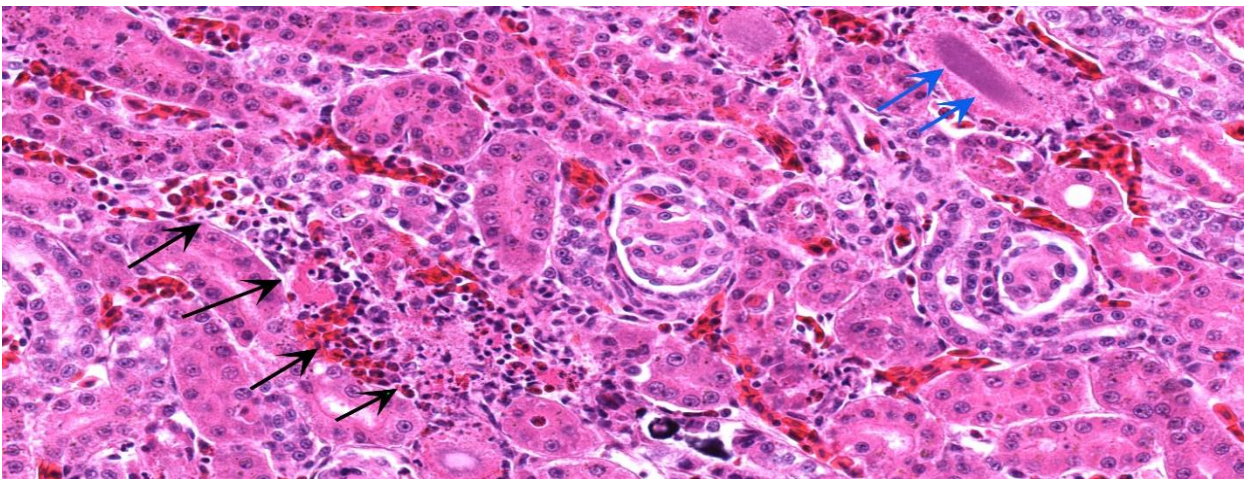
Figure 2-2. Kidney, penguin. There is multifocal tubular epithelial degeneration, necrosis, and sloughing into the lumen (black arrows). An adjacent degenerating tubule also contains crystalline mineral within the lumen. The lumen and epithelium of an adjacent tubule is effaced by spicular basophilic gouty tophi.

Lead Tissue Concentrations (Liver, Kidney)	Clinical Significance
<2mg/kg ww	Background level
2-6mg/kg ww	Subclinical poisoning
6-15mg/kg ww	Clinical poisoning
>15 mg/kg ww	Severe clinical poisoning and death
27 and 107 mg/kg ww	Chronic poisoning

Table 2

Contributor's Morphologic Diagnoses:
Kidney: Tubular degeneration and necrosis, multifocal, moderate with intranuclear acid-fast inclusion bodies, and intratubular urate crystal deposition.

Contributor's Comment:
Lead toxicosis is a well-recognized cause of morbidity and mortality in wildlife, humans and domestic animals. It is the most common form of heavy metal toxicity in birds, and is now thought to be the most frequent poisoning caused by a contaminant in avian species worldwide.[6] Common sources of lead exposure in birds include ammunition, fishing sinkers, coins, contaminated sed-

iment, as well as ingestion of affected animals (i.e. secondary poisoning).

Lead is capable of causing lesions and dysfunction in cardiovascular, neurological, hematopoietic, gastrointestinal, reproductive and immunological organs. Although the mechanism of lead-induced toxicity is not completely understood, the main targets of lead are enzymes involved in heme synthesis as well as thiol-containing antioxidants and enzymes (superoxide dismutase, catalase glutathione peroxidase, glucose 6-phosphate dehydrogenase, glutathione).[4] Low levels of lead in blood and tissue are sufficient to inhibit the activity of these enzymes, causing various effects, including impaired heme synthesis and generation of reactive oxygen
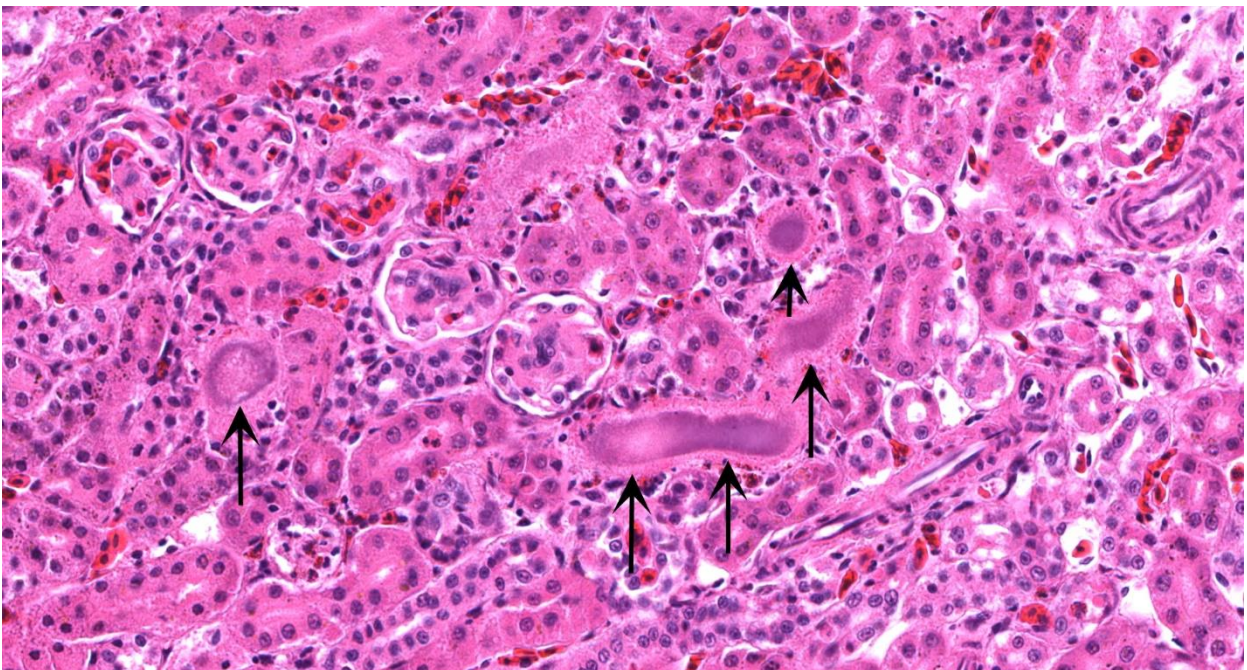

Figure 2-3. Kidney, penguin. Randomly scattered tubules are effaced by an aggregated of spicular basophilic gouty tophi (black arrows). (HE, 400X)

species (ROS). Additionally, lead inhibits and mimics the action of calcium, thus disrupting calcium-dependent pathways.

Generally, kidney and liver concentrations of lead above 36mg/kg on a dry weight basis are considered diagnostic for lead toxicosis in animals (per Puls, R. (1994) Mineral Levels in Animal Health. Diagnostic Data. 2nd Edition, Sherpa International, Clearbrook, 82.). Liver and kidney lead concentrations in this African Penguin were 48.24mg/kg and 289.5mg/kg, respectively, confirming lead toxicosis. Lead tissue concentrations (on a fresh weight base) and their clinical relevance in birds have also been reported (Table 2). Necropsy lesions can be absent or include pectoral atrophy, fat depletion, esophageal/ proventricular impaction, ventricular erosions, gallbladder distension and lead objects in gastric contents.[5] In the present case, the clinical presentation, pathology findings and toxicology results corroborate that this African penguin had a lead toxicosis. Due to the inhibition of heme synthesis, nonregenerative anemia is a common finding in lead toxicosis. Although this African penguin did not show profound anemia, the declining PCV was interpreted as a result of lead toxicosis. Notably, there were

histologic changes in the kidney that are characteristic of lead toxicosis, including epithelial cell degeneration in the proximal convoluted tubules and intranuclear acid-fast inclusions.[1]

Contributing Institution:
Johns Hopkins University, School of Medicine
Department of Molecular and Comparative Pathobiology
Broadway Research Building, #811
733 N. Broadway
Baltimore, MD 21205
Phone: 443-287-2953
Fax: 443-287-5628
http://mcp.bs.jhmi.edu/

JPC Diagnosis:
1. Kidney, tubules: Eosinophilic intranuclear inclusions.
2. Kidney, tubules: Nephritis, heterophilic, multifocal, mild, with gouty tophi and tubulorrhexis.
3. Liver, Kupffer cells and hepatocytes; kidney, tubular epithelium: Siderosis, diffuse, mild to moderate.
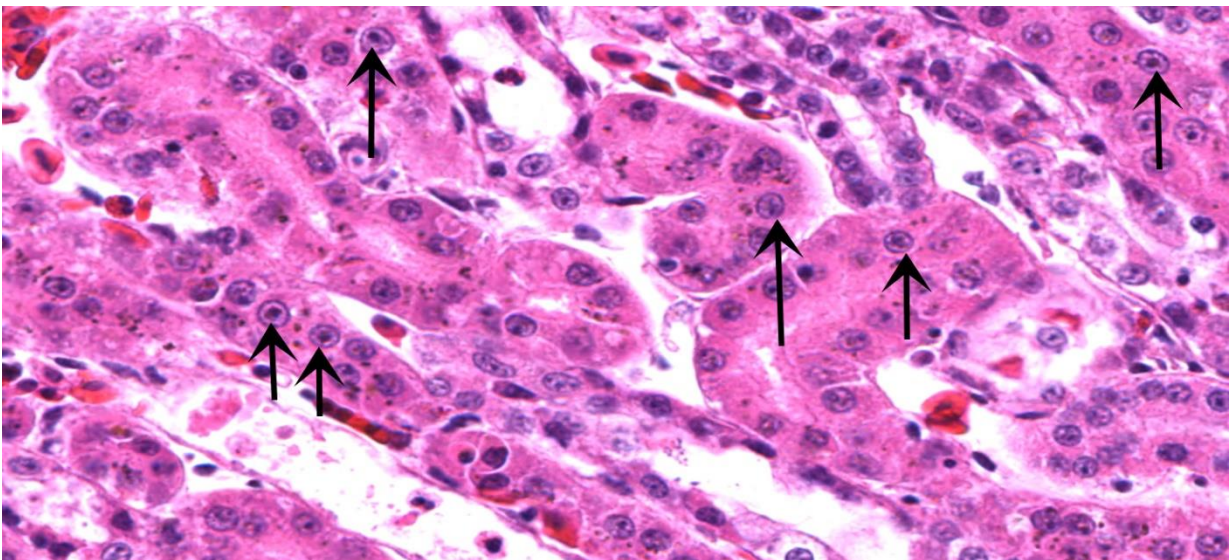

Figure 2-4. Kidney, penguin. Proximal convoluted tubule nuclei are occasionally enlarged by a 2-4 µm eosinophilic round lead inclusion surrounded by a clear halo. (HE, 460X)

JPC Comment:

The recognition of plumbism (i.e. lead poisoning) has a long history, with the oldest known written description attributed to the Greek physician Nicander during the second century B.C.E. Multiple notable Romans also wrote about the dangers of lead, including Pliny, who described the dangers of red lead and lead acetate while also describing how the leaching of copper into food could be prevented by lining copper pots with lead. He also endorsed the reduction of grape syrup in lead vessels to produce sapa, a syrup used to sweeten wine and preserve fruit, a process that inherently added lead acetate to the liquid.[2] Debate continues as to the role of lead in the fall of the Roman Empire, which is often attributed to the lead used in Roman water pipes. However, the main source of lead for the Romans was probably sapa.[2,7]

The primary route of entry of lead into the body is via the digestive tract. Fine particles of lead and lead salts are solubilized in the acidic environment of the stomach with most lead absorption occurring in the small intestine.[7] Inhaled fumes from heated lead and very fine particles (<0.5 µm) can enter the alveoli and be absorbed while larger particles are entrapped by the bronchial tree. These larger particles are then cleared from the airway by mucociliary action, swallowed,

Figure 2-5. Kidney, proximal convoluted tubules: Intranulcear inclusions stain positively with an acid-fast stain. (Ziehl-Neelsen, 400X)

and absorbed via the gastrointestinal tract. Risk factors for increased lead absorption include a high fat diet, mineral deficiency, and young age. High fat and mineral deficiency (e.g. calcium) can increase lead absorption by 7- and 20-fold, respectively. Non-ruminant animals absorb approximately 10% of dietary lead while ruminants absorb less than 3%. However, young animals can absorb up to 90%. Once absorbed, the majority of lead (60-90% depending on the species) is carried on the cell membrane of erythrocytes while the remainder is bound to protein or sulfhydryl compounds with only a scant amount found free in the serum. Lead is then distributed throughout the body, including crossing the blood-brain barrier, and accumulates in the active bone matrix (approximately 90%). Lead deposited in bone typically has a low turnover rate, however, it can be rapidly mobilized by lactation, pregnancy, or by the action of chelating agents.[7]

As noted by the contributor, lead toxicity commonly affects birds, including bald eagles. Plumbism in this species is primarily associated with the scavenging carcasses of animals killed with lead based ammunition and was found to be associated with 63.5% of diagnosed poisonings between 1975 and 2013 in a recent retrospective study.[3] Of 93 specimens with blood levels consistent with severe lead poisoning (≥1 ppm), gross lesions were most frequently observed in the heart (51/93 cases) with multifocal myocardial pallor and rounding of the apex. Gross lesions were also observed in the brain (19/93) with petechiae or hemorrhagic necrosis. Histologic lesions were most commonly noted within the heart (76/93), followed by the brain (59/93), and the eyes (24/87). Histologic lesions were characterized by fibrinoid necrosis of small to medium caliber arteries, predominantly within the previously identified organs, with the gross
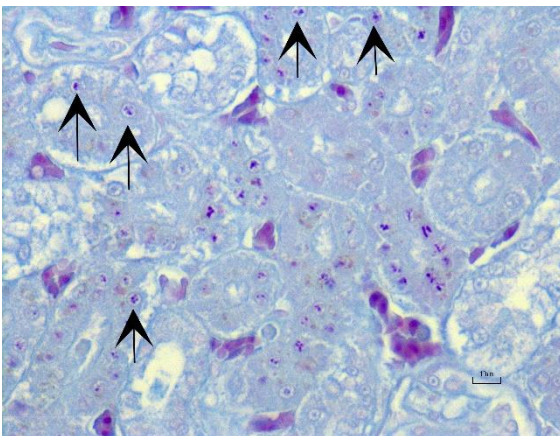
9

and histologic lesions consistent with ischemia caused by a primary vascular insult. As a result, the authors concluded the presence of these lesions in the absence of infectious agents or significant inflammation is suggestive of lead toxicity. Interestingly, renal tubular degeneration and necrosis was rare in bald eagles, and was minimal to mild when present. Intranuclear lead inclusion bodies were not detected in the afore-mentioned study. Definitive diagnosis of lead toxicity is preferably done utilizing liver and/or kidney tissue with liver lead concentrations greater than 6ppm (wet weight) thought to be associated with clinical toxicity and greater than 10ppm with severe poisoning in bald eagles, although levels less than 6 ppm were also found to be associated with severe or fatal lead toxicity.[3]

References:
1. Breshears MA and Confer AW. The Urinary System. In Pathologic Basis of Veterinary Disease. 6th Edition. Mosby Elsevier; 2017: 617-681.
2. Jonasson ME, Afshari R. Historical documentation of lead toxicity prior to the 20th century in English literature. *Hum Exp Toxicol*. 2018;37(8):775-788.
3. Manning LK, Wünschmann A, Armién AG, et al. Lead Intoxication in Free-Ranging Bald Eagles (Haliaeetus leucocephalus). *Vet Pathol*. 2019;56(2):289-299.
4. Nemsadze K et al. Mechanisms of lead-induced poisoning. Georgian Med News. Jul-Aug 2009; (172-173):92-6
5. Samour J. Toxicology. In Avian Medicine. 2nd edition. Mosby Elsevier; 2008: 269-281.
6. Stidworthy MF. And Denk D. Sphenisciformes, Gaviiformes, Podicipediformes, Procellariiformes and Pelecaniformes. In Pathology of Wildlife and Zoo Animals. 1st Edition. Academic Press; 2018: 653-686.
7. Thompson, LJ. Lead. In: Gupta RC, ed. *Veterinary Toxicology Basic and Clinical Principals.* New York, NY: Elsevier; 2007: 438-441

CASE III: 5239 (JPC 4135744)

Signalment:
Adult, female, guineafowl puffer (*Arothron meleagris*)

History:
This is a wild-caught, adult, female, guineafowl puffer that arrived into quarantine 6 months prior to presentation. The animal was placed into a 100,000 gallon mixed Indopacific teleost and elasmobranch exhibit after a 30-day period of quarantine. After 4 months on exhibit keepers reported decreased appetite, lethargy, self-isolation and possible intraspecific aggression toward the fish. The animal was transferred to a hospital tank for examination and treatment.

Examination revealed bilateral nodular, tan masses in the anterior chamber of the eyes, near the junction between the iris and sclera. Fine needle aspiration recovered numerous oval to round darkly staining, refractile
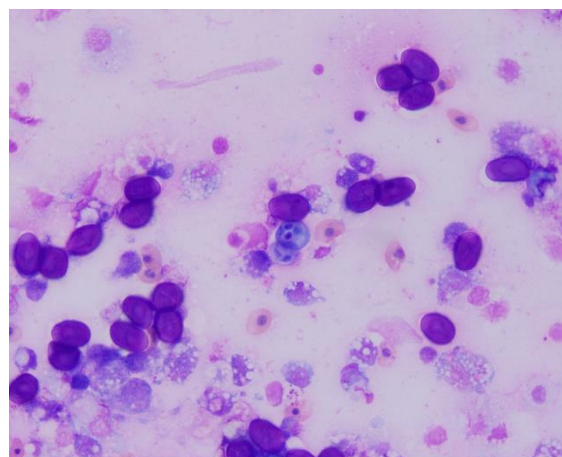

Figure 3-1. Cytology, anterior chamber, guineafowl puffer fish. There are numerous oval to round darkly staining, refractile structures intermixed with histiocytic and granulocytic inflammatory cells (*Photo courtesy of:* Wildlife Conservation Society, 2300 Southern Blvd., Bronx, NY 10460 https://www.wcs.org)

Figure 3-2. Swim bladder, guineafowl puffer fish. The mucosa is covered and the lumen is partially filled by a yellow-orange mucoid exudate. (*Photo courtesy of:* Wildlife Conservation Society, 2300 Southern Blvd., Bronx, NY 10460 https://www.wcs.org)

structures intermixed with histiocytic and granulocytic inflammatory cells. Acid-fast staining revealed these structures were strongly acid-fast with prominent bilateral polar capsules consistent with intraocular myxozoan infection. Ad-ditionally, the animal was negatively buoyant at exam and radiographs revealed a small asymmetrical/irregular swim bladder suggestive of concurrent aerocystitis. The animal was treated with injectable antibiotics, anti-inflammatories, and an oral gel diet containing amprolium for suspected bacterial aerocystitis and myxozoan-associated anterior uveitis/scleritis. The fish initially responded well to treatment, with improved appetite and activity, but acutely developed corneal clouding/edema and was found dead 4 weeks later.

Gross Pathology:
At necropsy, the swim bladder is intact, and the right lobe horn is approximately 20% smaller than the left horn. Adhered to the mucosal surface, and filling the lumen, is abundant, semi-firm, brown to yellow, waxy, material mixed with pale yellow to tan mucoid material and a small amount of red to brown, gelatinous to mucoid

material. Bilaterally, the eyes are mildly shrunken and the corneas are diffusely cloudy. Multifocally within the sclera and bulging onto the periocular surface of the left eye, are five, 0.4 cm to 0.6 cm in diameter, soft, pale yellow nodules, and one 0.5 cm in diameter soft, slightly flocculent dull red nodule. Multifocally within the sclera of the right eye and bulging into the periocular space are six, 0.4 cm to 0.6 cm in diameter, soft, pale yellow nodules, and one 1.0 cm in diameter soft, slightly flocculent dull red nodule.

Laboratory results:
No laboratory findings reported.

Microscopic Description:
Diffusely, the swim bladder mucosa is markedly expanded and largely effaced by multifocal to locally extensive, variably sized regions of necrosis and inflammation, and increased clear space (edema). Segmentally, the mucosal surface is ulcerated and replaced by a large sheet of epithelioid macrophages mixed with small numbers of lymphocytes and covered by a thick plaque of brightly eosinophilic necrotic material with pyknotic and karyorrhectic nuclear debris. Within the gas gland and rete mirabile and extending into the submucosa, are multifocal to locally
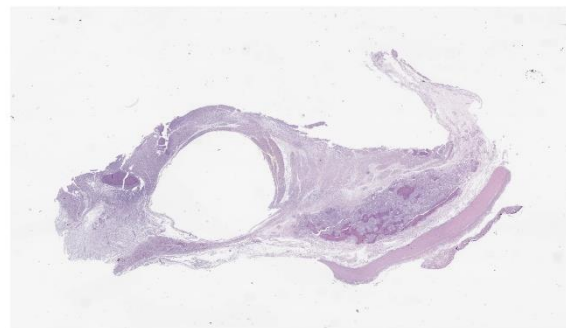
Figure 3-3. Swim bladder, guineafowl puffer fish. A section of swim bladder is submitted for examination. There as marked expansion of the wall of by numerous coalescing granulomas (upper left and lower right). The mucosa is multifocally ulcerated, and the external tunic is separated from the mural smooth muscle. (HE, 7X)

extensive, granulomas with variably thick layers of epithelioid macrophages, central brightly eosinophilic material with pyknotic and karyorrhectic nuclear debris or pale basophilic stippled material, and a peripheral rim of fibroblasts and occasional lymphocytes. Within these regions of necrotic debris as well as in the cytoplasm of intact macrophages are abundant negative staining, thin, bacilli. Also within regions of inflammation and in vessels, are small numbers of myxospores. Spores are ovoid to pyriform, approximately 10-12 um long and 8-10 um wide, with a refractile, 1um thick wall, two pyriform polar capsules oriented at one pole, and an occasionally visible, 1 um in diameter basophilic nucleus. The gas gland is moderately thickened up to 20-30 cell layers with multifocally hypertrophied epithelium up to 3x the normal cell size. Infiltrating the rete mirabile are small to moderate numbers of lymphocytes and histiocytes. Vessels are multifocally, mildly congested and frequently lined by plump endothelial cells. Scattered throughout the section are mildly increased numbers of rodlet cells. In some sections, there is a large round to oval region of clear space within the rete mirabile (presumed entrapped gas).

Contributor's Morphologic Diagnoses:
Swim bladder, Aerocystitis, granulomatous, necrotizing, multifocal to locally extensive, acute and chronic, severe with mucosal ulceration, edema, gas gland epithelial hyperplasia, and abundant intralesional and intrahistiocytic negative staining bacilli.

Swim bladder, Myxozoa, intravascular and intralesional, small numbers.

Contributor's Comment:
This case represents a chronic mycobacterial swim bladder infection with concurrent systemic myxozoa spread from a primary ocular myxozoan infection.

The swim bladder develops as a diverticulum of the pharynx, with either maintenance of a pneumatic duct between the swim bladder and the pharynx/esophagus in soft-rayed fishes (physostomes) or loss of the pneumatic duct in spiny-rayed fished (physoclistous).[3,7,8] The swim bladder's primary role is buoyancy, though it is also thought to play a role in sound reception/production and pressure reception.[3,8]

The swim bladder is commonly located in the dorsal 1/3 of the coelom, ventral to the posterior kidney and vertebral column, but the anatomy can vary between different species. The swim bladder can be ovoid or multilobulated, and may be one chamber (Salmonidae, Sygnathidae) or two chambers (Cyprinidae).[3,7,8] Wall thickness can also vary by species from thin and translucent to thick and opaque white. Histologically, the wall of the swim bladder is divided into four layers. The most internal layer, is the mucosa, which is comprised of single layer of cuboidal to transitional epithelium that is responsible for producing surfactant. The second layer is the muscularis, which can be composed of smooth muscle or skeletal muscle depending on the species, followed by the submucosa, which is composed of loosely arranged fibroblasts and collagen fibers that is also highly vascular. The most external layer is the external tunic, which is
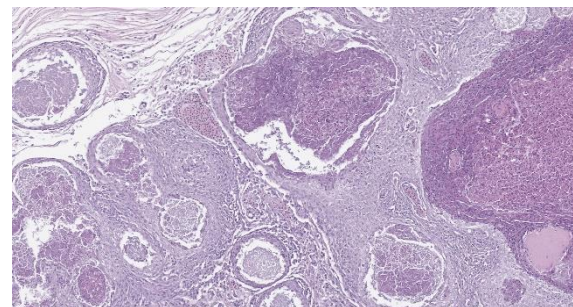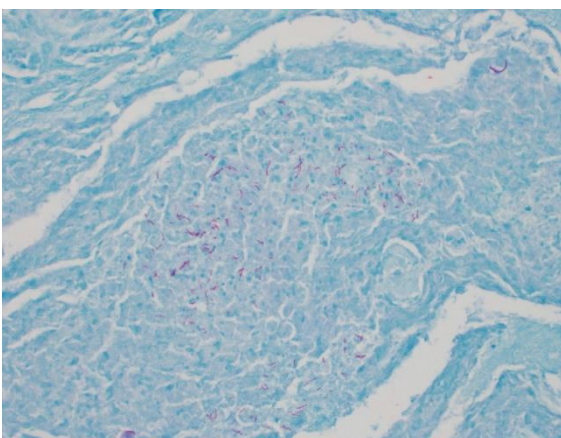

Figure 3-4. Swim bladder, guineafowl puffer fish. Numerous granulomas, some centered on eosinophilic cellular debris expand the wall of the swim bladder. (HE, 173X)

composed of compact fibroblasts and collagen bundles and a thin serosa.[3,8] There are three functional components to the swim bladder: the oval, the gas gland, and the rete mirabile.[3] The oval is on the caudodorsal wall of the swim bladder, and helps regulate oxygen movement from the lumen into the blood to reduce swim bladder volume.[3] The gas gland is located on the cranioventral aspect of the swim bladder and consists of a variably thick epithelial layer of gas gland cells responsible for acidifying the blood and releasing oxygen into the lumen.[2] Blood supply to the gas gland is provided by the rete mirabile, which is composed of many arterial and venous capillaries allowing for countercurrent blood flow.[3]

In the swim bladder of this guineafowl puffer, there was severe granulomatous and necrotizing inflammation with abundant acid-fast bacilli consistent with a Mycobacterium spp. *Carnobacterium maltaromaticum* and *Aeromonas hydrophila* were also cultured from the swim bladder, but these were considered a secondary infection and were not histologically apparent.
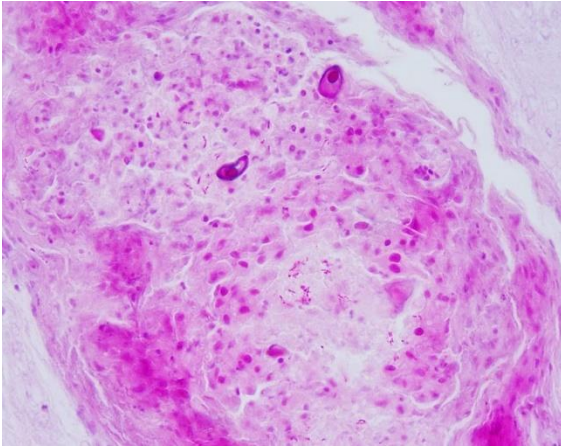

Figure 3-5. Swim bladder, guineafowl puffer fish. Small numbers of filamentous acid-fast bacilli are present within the center of the granulomas. (Ziehl-Neelsen, 400X)

Mycobacteriosis in fish often presents as a chronic disease for which clinical signs may not be observed. [4] Multiple non-tuberculous Mycobacterium species have been reported to cause disease in fish, though *M. marinum*, *M. chelonea* and *M. fortuitum* are reported as the most common isolates.[4] Systemic dissemination to multiple organs is common in fish mycobacteriosis, and associated inflammation is often granulomatous. Lesions can range from a mixture of macrophages and occasional granulocytes in acute lesions, to discrete granulomas with epitheloid macrophages centrally and a periphery of fibroblasts and lymphocytes in more chronic lesions.

This fish also had a severe, bilateral ocular myxozoan infection, and on histopathologic examination, myxospores were noted in the swim bladder, vessels in the wall of the gastrointestinal tract, and melanomacrophage centers in the spleen and anterior kidney, supporting systemic spread. The myxozoa were not considered to be a primary cause of inflammation in the swim bladder, and likely colonized the region opportunistically. At the time of submission, a definitive identification of the myxozoan was not available; however, based on the cytologic appearance of the organisms and histologic lesions centered on the scleral cartilage in the eyes, a *Myxobolus* spp. was considered most likely.

While some species of myxozoans, such as *Myxobolus cerebralis*, *Henneguya ictaluri*, and *Tetracapsuloides bryosalmonae*, are known to cause significant clinical disease, many infections are subclinical.[1,6] However, if myxozoan cysts rupture, the release of the spores and can incite a local inflammatory response and occasionally involve other organ systems.[1,6] Presumably, this fish arrived into quarantine with a subclinical ocular myxozoan infection, and it was not

Figure 3-6. Swim bladder, guineafowl puffer fish. Granulomas occasionally contain one or multiple elliptical to oval myxospores. (PAS, 400X)

until the myxozoan cysts ruptured that clinical signs and grossly apparent ocular lesions manifested.

Contributing Institution:

Wildlife Conservation Society
2300 Southern Blvd.
Bronx, NY 10460
https://www.wcs.org

JPC Diagnosis:

1. Swim bladder, mucosa and submucosa: Aerocystitis, granulomatous, multifocal to coalescing, severe, with ulceration, intravascular gas bubble formation, rodlet cell hyperplasia, and gas gland hyperplasia and hypertrophy.

2. Swim bladder, granulomas and rete mirabile: Myxospores, numerous.

JPC Comment:

The contributor provides an excellent review of the development, anatomy, physiology, and roles associated with the swim bladder in various fish species as well as an overview of mycobacteriosis and myxozoans.

Mycobacteriosis in fish was first described in carp (*Cyprinus carpio)* by Bateaillon et al. in 1897. As noted by the contributor, three

Mycobacterium spp. have since dominated the literature in regard to fish: *Mycobacterium marinum*, *Mycobacterium fortuitum*, and *Mycobacterium chelonae*.[4]

Pathogenic mycobacteria are predominately intracellular organisms found within phagocytes that are resistant to the normal processes of acidification and phagolysosomal fusion. In addition, pathogenic mycobacteria are thought to retard the maturation of mammalian phagosomes and their progression to the phagolysosomal state by preventing fusion with components of the late, but not early endosomal network. Furthermore, *M. marinum* in mouse macrophages has been shown to escape phagosomes and spread directly from cell to cell via actin-based motility. However, less information exists in regard to the behavior of mycobacteria within poikilotherm macrophages. Using cell lines derived from carp leukocytes, *M. marinum* was found to inhibit phagolysosome fusion. However, phagolysosome fusion occurred in vivo in striped bass infected with *M. marinum*, with similar findings in frog and fish tissues. These findings suggest multiple intracellular survival strategies may be used by these intracellular bacteria in poikilotherms.[4]

External clinical signs are non-specific and include scale loss, dermal ulceration, pigmentary changes, abnormal behavior, spinal defects, emaciation, and ascities. Gross internal lesions include enlargement of the spleen, kidney, and liver, and characteristic grey or white nodules on internal organs.[4]

A recent report described a continuum of variably mature granulomatous lesions caused by *Mycobacterium chelonae* in two farmed Japanese pufferfish (*Takifugu rubripes*) within the swim bladder, kidney, spleen, and gills.[5] The most mature lesions comprised of encapsulated granulomas with

14

central necrosis were most commonly identified in the swim bladder. Intermediate lesions with encapsulated granulomas without central necrosis and immature lesions with unencapsulated clusters of epithelioid macrophages were most frequently identified in the kidney and spleen, and the gills most commonly exhibited immature lesions. The presence mature granulomas in the swim bladder in comparison to other locations suggested that *M. chelonae*-induced lesions in the swim bladder either formed earlier during the infection (i.e. the swim bladder was more susceptible to infection), or *M. chelonae* induced lesions developed more rapidly in the swim bladder compared with other organs. Given that the swim bladder is composed primarily of oxygen, the authors of the report suggest the association of the mature lesions with the swim bladder may have been due to the typically aerobic nature of *Mycobacterium* spp., as well as the organ's connection to the circulatory system with a rich blood flow.[5] As noted by the contributor, multiple non-tuberculous Mycobacterium species have been reported to cause disease in fish.[5]

In this case, acid fast stains (Fite-Faraco and Ziehl-Neelsen) reveal small numbers of filamentous acid-fast bacilli within multifocal granulomas. Although these findings are consistent with *Mycobacterium* spp., results of confirmatory testing such as PCR, if performed, were not included in the WSC submission.

Myxozoans are metazoan parasites that predominantly infect poikilothermic animals, with over 700 species described in fish. These parasites have a complex life-cycle that often alternates between vertebrate and invertebrate hosts with sporogony occurring in each (i.e. alternated bisporogony). As noted by the contributor, the majority of infections cause chronic subclinical disease with little to no clinical signs or host immune response. However notable exceptions associated with high morbidity and mortality and significant economic loss include *Myxobolus cerebralis*, *Henneguya ictaluri*, and *Tetracapsuloides bryosalmonae*, the species associated with whirling disease of the salmon, proliferative gill disease of the catfish, and proliferative kidney disease of salmon, respectively. Although predominantly considered a disease of farmed fish, whirling disease has been found in wild stock, raising concerns in regard to population decline.[1]

References:

1. Cavin JM, Donahoe SL, Frasca S, et al. Myxobolus albi infection in cartilage of captive lumpfish (Cyclopterus lumpus). *JVDI*. 2012;24(3):516–524.
2. D'Aoust BG. The role of lactic acid in gas secretion in the teleost swimbladder. *Comp Biochem Physiol*. 1970;32: 637–668.
3. Fange R. Physiology of the swimbladder. *Physiol Rev*.1966;46:299–322.
4. Gauthier DT and Rhodes MW. Mycobacteriosis in fishes: A review.*The Vet Jou*r.2009;180(1): 33-47.
5. Ishii Y, Kawakami H, Mekata T, Sugiyama A. Histopathological Features of Mycobacterium chelonae Infection in Two Farmed Japanese Pufferfish (Takifugu rubripes). *J Comp Pathol*. 2019;170:86-90.
6. Kent, ML, Andree, KB, Bartholomew, JL Recent advances in our knowledge of the Myxozoa. J Eukaryot Microbiol. 2001;48:395–413.
7. Lumsden, JS. Gastrointestinal tract, swim bladder, pancreas and peritoneum. In: Ferguson HW, ed. *Systemic Pathology of Fish*. London, UK: Scotian Press; 2006: 169-199.

8. Roberts, RJ. 2012. The anatomy and physiology of teleosts. In: Roberts RJ, ed. *Fish Pathology*, 4th ed. West Sussex, UK: Blackwell Publishing, Ltd; 2012:17-61.
9. Roberts, RJ. 2012. The pathophysiology and systematic pathology of teleosts. In: Roberts RJ, ed. *Fish Pathology*, 4th ed. West Sussex, UK: Blackwell Publishing, Ltd; 2012: 62-143.

CASE IV: M20-05667 (JPC 4155412)

Signalment:
12 month old, mixed sex, diploid Sydney Rock Oysters (*Saccostrea glomerata*)

History:
A mortality event of approximately 42% occurred on an oyster farm in autumn, with the worst affected oysters being the oldest, and those positioned on floating baskets compared with the lesser affected intertidal baskets. Water quality at the time was described as the 'worst in over 50 years', persisting since heavy rains caused flood events after the area was impacted by large bush fires in Summer 2019-2020. Dead oysters presented as empty shells, and farmers noted remaining oysters were weaping a clear liquid.

Gross Pathology:
12 oysters were opened and examined. Most of the oysters appeared watery, with pale digestive glands. Non-affected oysters presented with normal dark brown digestive gland.

Laboratory results:
The digestive gland of each oyster was examined with impression smear, stained with Diff Quick. A sample of digestive gland was also collected and a QX (*Marteilia sydneyi*) PCR was performed. A strong correlation between smear results and DNA PCR results is consistently observed in our laboratory.

Microscopic Description:
Impression smears, digestive gland, Sydney rock oysters.

There is moderate background granularity and amorphous debris. The smears contain nuclear material in streaks or clusters, and abundant sperm. There are numerous digestive gland epithelial cells with mild
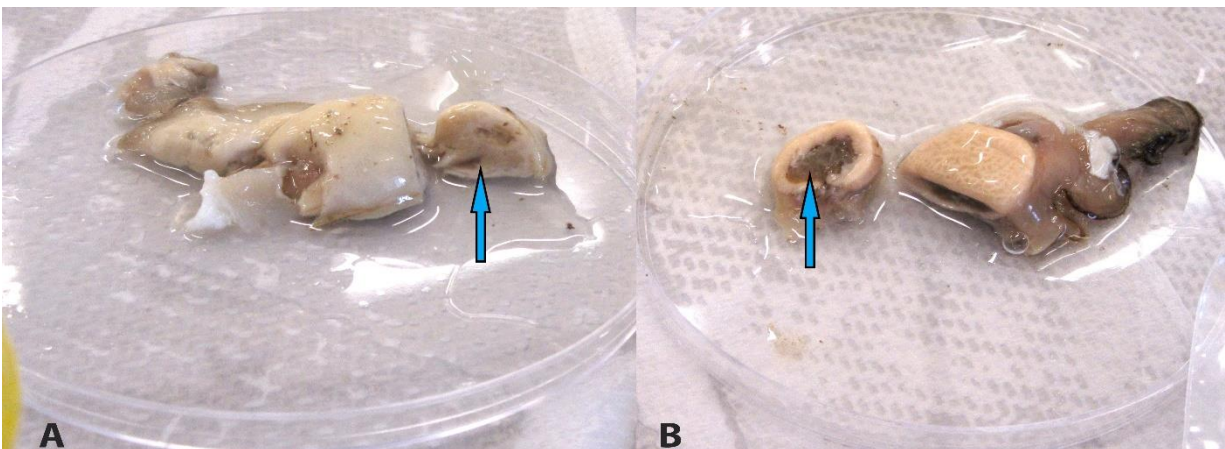
Figure 4-1. Presentation, Sydney rock oysters. Affected oysters appeared watery, with pale digestive glands (left). Non-affected oysters presented with normal dark brown digestive gland (right). *Photo courtesy of:* **Elizabeth Macarthur Agricultural Institute, Woodbridge Road, Menangle NSW 2568 Australia, https://www.dpi.nsw.gov.au/about-us/services/laboratory-services)**

variation in size between 15-25µm, with large pale vacuolated cytoplasm and a loosely stained single nuclei. Occasionally there are basophilic secretory cells present, with dark blue cytoplasm and smaller size (approximately 5-10 µm diameter), and rare hemocytes. There are numerous various protozoal life cycle stages, including daughter cells (small 5-10 µm oval cells with blue cytoplasm), daughter cells containing secondary cells (larger 10-15 µm containing one or more plasmodia), immature sporonts and mature sporonts (containing numerous blue refractile bodies and two spores), admixed with cellular debris and ruptured nurse cells (sporangiosori).

Contributor's Morphologic Diagnoses:
Digestive gland smear: Marked parasitism with ruptured nurse cells, consistent with *Marteilia sydneyi* infection, Sydney rock oyster (*Saccostrea glomerata*).

Contributor's Comment:
The Australian bushfires in the summer of 2019-2020 burnt over 4.9 million hectares of land in New South Wales. Almost immediately following this event, there were heavy rainfalls, resulting in abundant ash runoff into rivers and estuaries. This ash

particulate matter, combined with the fluctuations in salinity associated with flooding, may have contributed to many reports of mortalities in farmed aquaculture species, including the Sydney rock oysters, during this time. This mortality event was located in an estuary previously known to have QX, however active disease in Sydney rock oysters had not been diagnosed in the area for 13 years.

QX disease is caused by a protozoan parasite, *Marteilia sydneyi* (phylum Paramyxea).[5] The organism has been shown to have another host and potential environmental reservoir, the polychaete worm *Nephtys australiensis.*[1] Since there is an environmental reservoir for the organism, it may be years between disease outbreaks in estuaries where the parasite is endemic.

Death from QX disease generally occurs in late summer to early spring (February-September)[6] and may be associated with heavy rainfall[3] and low salinity.[4] Disease is diagnosed when the organism reaches sporulation in the digestive gland of Sydney rock oysters, thereby creating massive digestive gland lysis, necrosis and subsequent starvation and death of the
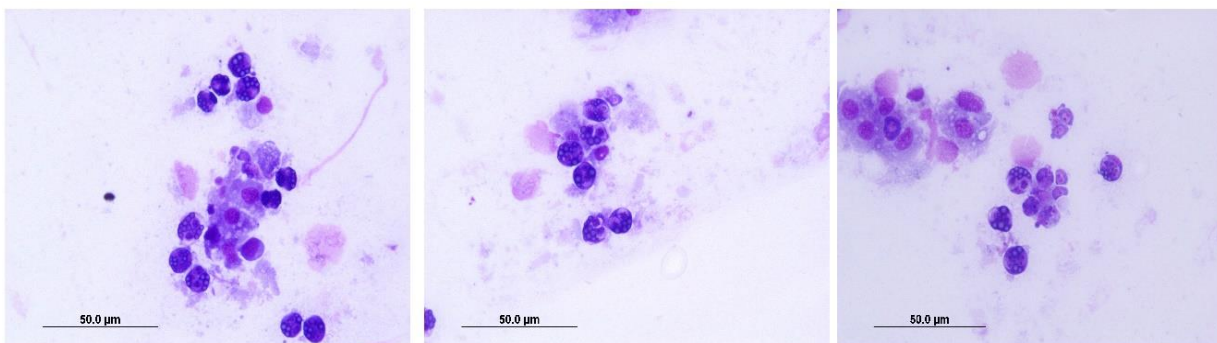

Figure 4-2. Digestive gland, Sydney rock oysters. There are numerous digestive gland epithelial cells with large pale vacuolated cytoplasm and a loosely stained single nuclei. Within many of these cells, there are numerous various protozoal life cycle stages, including daughter cells (small 5-10 µm oval cells with blue cytoplasm), daughter cells containing secondary cells (larger 10-15 µm containing one or more plasmodia), immature sporonts and mature sporonts (containing numerous blue refractile bodies and two spores), admixed with cellular debris and ruptured nurse cells (sporangiosori) *Photo courtesy of:* Elizabeth Macarthur Agricultural Institute, Woodbridge Road, Menangle NSW 2568 Australia, https://www.dpi.nsw.gov.au/about-us/services/laboratory-services

oyster.[6] Infected farms usually discover empty shell (dead oysters), with diseased oysters having pale, swollen digestive glands on gross examination. Individuals may also have depleted glycogen storage and gonad, with an overall watery appearance.[6]

Since *M. sydneyi* is present and endemic in a number of waterways in NSW, the diagnosis of disease requires the detection of sporulating forms, therefore digestive gland smear and histology is required to form a diagnosis. The detection of DNA alone by PCR is not a confirmatory test for the presence of disease. Digestive gland smears, stained with Diff Quick, are a relatively cost effective, fast and reliable diagnosis method, when compared with PCR or histopathology. In a study involving eighty oysters, results indicated cytology of digestive gland impression smears (96.88%) had a greater sensitivity of detecting QX disease than histology (86.11%).[2]

Contributing Institution:
https://www.dpi.nsw.gov.au/about-us/services/laboratory-services

JPC Diagnosis:
Impression smear, digestive gland: Epithelial cell degeneration with numerous intracellular sporonts consistent with *Marteilia* sp

JPC Comment:
Disease has been the predominant controlling factor in oyster population dynamics since the development of oyster farming. Based almost entirely upon only five species, global oyster production typically occurs in monocultures inherently vulnerable to disease epizootics. Other than OsHV1 in Pacific oysters, the majority of oyster diseases are caused by protozoan parasites, including both QX disease and Winter Mortality Syndrome in Sydney rock oysters (*Saccostrea glomerata*).[6]

Sydney rock oyster farming is the fourth largest oyster aquaculture industry in the world and is New South Wales' largest aquaculture industry. However, production has declined over 40% since the 1970s, primarily due to the two aforementioned diseases. This trend has continued, with 3843 tons of edible oysters harvested in 2010-2011, 22% less ($4.7 million) than the previous year.

QX (for Queensland Unknown) disease, also known as marteilosis, is the most serious of the two diseases with mortality rates reported to be ≥95% in some outbreaks.[1,6] Outbreaks of QX disease caused by *Marteilia sydneyi* were first identified in the late 1970's and described by Perkins and Wolf in 1976.[6]

The earliest infectious stage of *M. sydneyi* that can be identified in oysters is a uninucleate stem cell discovered in the palps and gill epithelia of rock oysters (*Saccostrea glomerata*), suggesting infection results from a "free floating" parasitic stage entering the gills during filter feeding followed by proliferation in the gill epithelium. Once sufficient numbers of stem cells are generated, they penetrate the basal membrane, enter connective tissue, and disseminate throughout the oyster with the majority found in the digestive gland within the digestive tubule epithelium. Replication continues within the digestive gland, forming a 2-celled plasmodium that further divides to form between 8 and 16 sporonts. Sporonts undergo additional internal division to form two spores, each with three concentric cells. These spores are then shed into the environment via the alimentary canal prior to the death of the oyster.[6]

The lifecycle of *M. sydneyi* once shed from infected oysters is unclear. Spores are relatively short-lived outside the oyster host (7-35 days) compared to the 3-10 month infection cycle of the pathogen within the host, supporting the theory of an intermediate host in the lifecycle of *M. sydneyi*.[6] As noted by the contributor, previously unidentified and different morphologic stages of *M. sydneyi* have recenly been identified within *Nephtys australiensis,* one of many polychaete nematodes found within the sediment near oyster leases. Although additional study is needed, it is possible the rock oyster and *N. australiensis* are the only two hosts required for the life cycle of this parasite.[1]

Winter Mortality Syndrome, the second major protozoan disease of Sydney rock oysters is caused by *Bonamia roughleyi*. As its name suggests, this disease predominantly occurs during the cooler months from June to August and is restricted to the cooler southern range of rock oysters. Mortality rates of up to 80% are common in affected areas and oysters are most susceptible in their third winter, just prior to reaching market size.[6]

References:

1. Adlard RD, Nolan MJ. Elucidating the life cycle of Marteilia sydneyi, the aetiological agent of QX disease in the Sydney rock oyster (*Saccostrea glomerata*). *Intern. J. Parasitol*. 2015 March 45; 419-426.
2. Adlard RD, Wesche SJ. Aquatic Animal Health Subprogram: Development of a disease zoning policy for *Marteilia sydneyi* to support sustainable production, health certification and trade in Sydney rock oyster. Fisheries Research and Development Corporation. Queensland Museum. 2005 2001/214.
3. Anderson TJ, Wesche S, Lester RJG. Are outbreaks of *Marteilia sydneyi* in Sydney rock oysters, *Saccostrea commercialis*, triggered by a drop in environmental pH? *Aust. J. Marine Freshwater Res*. 1994 45;1285-7.
4. Butt D, Shaddick K, Raftos D. The effect of low salinity on phenoloxidase activity in the Sydney rock oyster, *Saccostrea glomerata*. *Aquaculture*. 2006 251; 159-166.
5. Perkins FO, Wolf PH. Fine structure of *Marteilia sydneyi* sp. n. – Haplosporidian pathogen of Australian oysters. *J. Parasitol.* 1976 August 62;4:528-538.
6. Raftos DA, Kuchel R, Aladaileh S, Butt D. Infectious microbial diseases and host defense responses in Sydney rock oysters. *Front Microbiol*. 2014;5:135. Published 2014 Apr 23.
7. Wolf PH. Life cycle and ecology of *Marteilia sydneyi* in the Australian oyster, *Crassostrea commercialis*. *Marine Fisheries Review*. 1979 41(1-2) 70-2.